JOURNAL OF VIROLOGY, Apr. 1978, p. 71-83
0022-538X/78/0026-0071$02.00/0

Vol. 26, No. 1
Printed in U.S.A.

Mapping Host Range-Specific Oligonucleotides Within Genomes of the Ecotropic and Mink Cell Focus-Inducing Strains of Moloney Murine Leukemia Virus

THOMAS Y. SHIH,[1]* MAUREEN O. WEEKS,[1] DAVID H. TROXLER,[1] JOHN M. COFFIN,[2] AND EDWARD M. SCOLNICK[1]

Laboratory of Tumor Virus Genetics, National Cancer Institute, National Institutes of Health, Bethesda, Maryland 20014,[1] and Department of Molecular Biology and Microbiology, Tufts University School of Medicine, Boston, Massachusetts 02111[2]

Received for publication 14 November 1977

The site of recombination of a mink cell focus-inducing strain (Mo-MuLV$_{83}$) derived from an ecotropic Moloney murine leukemia virus (Mo-MuLV) was mapped by fingerprint analysis of the large RNase T1-resistant oligonucleotides, employing a two-dimensional gel electrophoresis method. Mo-MuLV$_{83}$, in contrast to the ecotropic Mo-MuLV, demonstrated a broadened host range, i.e., growth not only on mouse cells but also on mink cells, and recombination involved the *env* gene function. The genomic RNA of these two viruses shared 42 out of a total of 51 to 53 large T1 oligonucleotides (81%) and possessed a similar subunit size of 36S. Most of these T1 oligonucleotides were mapped in their relative order to the 3′ polyadenylic acid end of the viral RNA molecules. There were 10 common oligonucleotides immediately next to the 3′ termini. A cluster of 7 (in Mo-MuLV$_{83}$) or 10 (in Mo-MuLV) unique T1 oligonucleotides were mapped next to the common sequences at the 3′ end, and they all appeared concomitantly in a polyadenylic acid-containing RNA fraction with a sedimentation coefficient slightly larger than 18S. Therefore, the *env* gene of Mo-MuLV was situated at a location approximately 2,000 to 4,000 nucleotides from the 3′ end of the genomic RNA, and the gene order of Mo-MuLV appeared to be similar to that of the more rigorously determined avian oncornaviruses. cDNA$_{SFFV}$ specific for the xenotropic sequences in the spleen focus-forming virus RNA hybridized to the cluster of unique oligonucleotides of Mo-MuLV$_{83}$ RNA. This suggests that the loci of recombination involve the homologous *env* gene region of a xenotropic virus.

Four genetic functions have been defined in RNA tumor viruses: (i) the *gag* gene codes for internal structural proteins of the virion; (ii) the *pol* gene specifies the reverse transcriptase; (iii) the *env* is the genetic function determining host range properties for the viruses and codes for envelope glycoproteins; and (iv) in avian sarcoma viruses, a *sarc* gene is responsible for malignant transformation of normal cells (1, 9, 22). Although a complete genetic map following the 5′ to 3′ direction in the order of *gag-pol-env-sarc*-polyadenylic acid [poly(A)] within the genomic viral RNA has been determined in avian sarcoma viruses (5, 13, 24), a similarly rigorous genetic map of mammalian RNA tumor viruses is still lacking.

In the course of studies in this laboratory involving the spleen focus-forming virus (SFFV) of the Friend leukemia virus complex, cloned isolates of replicating murine leukemia virus (MuLV) were found to have a broadened host range, allowing growth on both mouse cells and cells permissive for xenotropic viruses (21). Of special interest among these isolates is a Moloney murine leukemia virus clone 83 (Mo-MuLV$_{83}$), which demonstrates such a broadened host range. In contrast to the ecotropic Moloney murine leukemia virus (Mo-MuLV), it grows not only on mouse cells but also on mink lung fibroblasts and induces the typical cytopathic foci of mink cell focus-forming viruses (MCF viruses) (10). Mo-MuLV$_{83}$ appears to be a recombinant between the ecotropic Mo-MuLV and a xenotropic MuLV because of the following observations: (i) the xenotropic sequences in Mo-MuLV$_{83}$ are detectable by a cDNA probe, which represents a xenotropic portion of SFFV (cDNA$_{SFFV}$); (ii) the interference pattern of virus infection between MuLV's and challenging Kirsten sarcoma virus pseudotypes of MuLV's shows that Mo-MuLV$_{83}$ is interfered with by both xenotropic and ecotropic viruses. Thus, the

loci of recombination of Mo-MuLV$_{83}$ involve the *env* gene function (21).

We have attempted to map the site of recombination and the location of the *env* gene function within the MuLV genome. In a previous study (21), cDNA$_{SFFV}$ detecting the xenotropic sequences was found to hybridize most rapidly to a piece of Mo-MuLV$_{83}$ poly(A)-containing RNA of 18 to 26S in size. To further compare the genome of these two viruses, large RNase T1-resistant oligonucleotides were fingerprinted by a two-dimensional gel electrophoresis method that we used previously to map the Kirsten sarcoma virus genome (17). The physical map of the large T1 oligonucleotides of these two viruses demonstrated a cluster of 7 to 10 unique T1 oligonucleotides located approximately 2 to 4 kilobases (kb) from the 3′ end of the genomic RNA. cDNA$_{SFFV}$ thus appears to detect the *env* gene region of a xenotropic virus.

MATERIALS AND METHODS

Cells and viruses. Mo-MuLV$_{83}$ was isolated in this laboratory by end-point dilution cloning in Microtest II culture plates on a wild mouse embryo fibroblast cell line (SC-1) from a stock of Mo-MuLV originally obtained from Robert Bassin (National Cancer Institute, Bethesda, Md.) (21). It had acquired broadened host range through recombination with a murine xenotropic virus and was propagated on a mink lung fibroblast cell line to avoid contamination by other ecotropic viruses. Mo-MuLV clone 2 was obtained from Nancy Hopkins (Massachusetts Institute of Technology, Cambridge, Mass.) and was originally cloned by Fan and Baltimore (6, 14). It was propagated on SC-1 cells. All cells were grown in Dulbecco-Vogt modified Eagle minimal essential medium supplemented with 10% calf or fetal calf serum (GIBCO). All cells were monitored for mycoplasma by both aerobic and anaerobic techniques and were found to be negative.

Preparation and fingerprinting of viral RNA. ^{32}P labeling of viral RNA and fingerprinting of the labeled RNA by two-dimensional gel electrophoresis were as previously described (17). Short-term labeling with [^{3}H]uridine or [^{32}P]orthophosphate for subunit size determination is described in the legend to Fig. 2. Composition of pancreatic RNase A digests was analyzed as described previously (3).

Deduction of the physical map of RNase T1-resistant oligonucleotides. Deduction of the physical map of RNase T1-resistant oligonucleotides was essentially as reported previously (3, 17, 23). Briefly, viral RNA either naturally or further chemically degraded by treatment with Na_2CO_3 was sedimented on a sucrose density gradient. Pools were made encompassing molecules of ±2 to 4S in size. Poly(A)-containing RNA fragments were then isolated by two cycles of oligodeoxythymidylic acid$_{12\text{-}18}$ [oligo(dT)$_{12\text{-}18}$]-cellulose chromatography and were fingerprinted after complete digestion with RNase T1. Since most of the fingerprints obtained under our present experimental conditions overlap very well, corresponding T1 oligonucleotides can be readily identified by direct superimposition of these fingerprints. The order of RNase T1-resistant oligonucleotides within the genomic viral RNA was determined first by visual inspection of the fingerprints. Assuming that poly(A) tracts were at the 3′ end of the RNA molecules, T1 oligonucleotides, which were present in large but absent in smaller size poly(A)$^+$ RNA fragments, were placed at location close to the 5′ end of the genome, and oligonucleotides remaining in the smallest size fraction were at the 3′ end. The order of T1 oligonucleotides within each size fraction was further determined by recovery of T1 oligonucleotides in the second-dimension gel. Oligonucleotides with higher relative molar yield were placed proximal to the 3′ end of the genome. The first visual inspection in the present two-step procedure enables one to discern more precisely the partially separated oligonucleotides, and any major discrepancy in the entire fingerprint can be discovered.

RNA-DNA hybridization. cDNA$_{SFFV}$ specific for the xenotropic sequences in SFFV was prepared as follows: cDNA was prepared from an SFFV-Friend helper type C virus (F-MuLV) pseudotype released from a Fisher rat embryo cell; the F-MuLV sequences were then removed by absorption on a hydroxyapatite column after hybridization of cDNA with an excess of F-MuLV RNA (20). Protection of the T1 oligonucleotides of [^{32}P]Mo-MuLV$_{83}$ RNA by cDNA$_{SFFV}$ was performed as described previously (17). Briefly, after hybridization of [^{32}P]Mo-MuLV$_{83}$ RNA to cDNA$_{SFFV}$ (RNA was in slight excess), it was digested with a combination of pancreatic RNase A and RNase T1. After heat dissociation, the portion of [^{32}P]Mo-MuLV$_{83}$ RNA protected by cDNA$_{SFFV}$ was further digested with RNase T1 and fingerprinted.

RESULTS

Comparison of fingerprints of Mo-MuLV$_{83}$ and Mo-MuLV RNA. The 60–70S viral RNA of Mo-MuLV$_{83}$ and Mo-MuLV has been analyzed by the two-dimensional gel electrophoresis method after complete digestion of the [^{32}P]RNA with RNase T1. The first-dimension gel (10% acrylamide–6 M urea, pH 3.5) separates T1 oligonucleotides according to their protonated adenine plus cytosine content in addition to their chain length, and the second-dimension gel (21.8% acrylamide, pH 8.0) resolves oligonucleotides primarily according to the chain length. Representative fingerprints of Mo-MuLV$_{83}$ and Mo-MuLV are seen in Fig. 1A and C. It is evident by superimposition of these two fingerprints that most of the T1 oligonucleotides of these two viruses possessed similar electrophoretic mobility, as indicated by the dark spots of the sketches of fingerprints (Fig. 1B and D). To further ascertain this point more accurately, [^{32}P]RNAs of Mo-MuLV$_{83}$ and Mo-MuLV were mixed at ratios of 3:1, 1:1, or 1:3, and they were fingerprinted. Figure 1E shows the fingerprint of the mixture of these two viral

RNAs at a ratio of 1:1. As expected, the pattern looked very much similar to fingerprints of these two viruses alone, and all the common oligonucleotides coelectrophoresed as the dark spots in the mixture. Another type of double-labeling experiment involved coelectrophoresis of [^{32}P]-Mo-MuLV$_{83}$ RNA and Mo-MuLV RNA labeled with [5,6-^{3}H]uridine in vivo, which incorporated the ^{3}H label in both uridine and cytosine residues of viral RNA (4). After complete RNase T1 digestion of the viral RNA mixture, oligonucleotides were separated in the two-dimensional gel and located by the ^{32}P label of Mo-MuLV$_{83}$ RNA in the autoradiograph. Gel disks (5 mm in diameter) were excised out of the second-dimension gel, and the radioactive oligonucleotides were eluted and counted. The ^{3}H-^{32}P ratio of Mo-MuLV$_{83}$ spots is seen in Table 1. All the T1 oligonucleotides common between these two viruses possessed a ^{3}H-^{32}P ratio close to the normalized value of 1.0 (0.57 to 1.54). Some variation in the ^{3}H-^{32}P ratio may reflect differences in base composition or overlapping and incomplete resolution of these T1 oligonucleotides. It is clear that the unique spots of Mo-MuLV$_{83}$ such as A3, A5, A11, A25, A26, and A33 all showed lower ^{3}H-^{32}P ratios (0.07 to 0.39). An exception in spots A20 and A31 (^{3}H-^{32}P ratios of 1.30 and 1.03) was due to incomplete resolutions of these oligonucleotides (Fig. 1F). Composition analysis of pancreatic RNase A digests of T1 oligonucleotides is also shown in Table 1. Most of the common oligonucleotides possessed similar composition as those of Mo-MuLV RNA, and unique oligonucleotides possessed unique composition. Composition of no. 8 oligonucleotides differed between these two viruses, although electrophoretic mobility was very close. Thus, by the above criteria, 42 out of 51 numbered oligonucleotides of Mo-MuLV$_{83}$ (82%) and 42 out of 53 of Mo-MuLV spots (79%) were common between these two viruses. These RNase T1-resistant oligonucleotides represent approximately 10% of the total viral RNA, and the present results strongly suggest that 79 to 82% of the genome of these two viruses are identical in their nucleotide sequences.

Subunit size of Mo-MuLV$_{83}$ RNA. To examine the size of Mo-MuLV$_{83}$ RNA as compared with that of Mo-MuLV, the following double-labeling experiments were performed. Mo-MuLV$_{83}$ RNA was labeled with [^{32}P]orthophosphate, and Mo-MuLV was labeled with [^{3}H]uridine. Media from these two cell cultures were pooled, and viruses were pelleted by high-speed centrifugation. The 60 to 70S viral RNA was sedimented through the sucrose density gradient after disruption of the virion in the detergent. As seen in Fig. 2A, the native dimer structure of Mo-MuLV$_{83}$ sedimented at 60S as compared with the 70S Mo-MuLV RNA. However, upon heat denaturation of the viral RNA complexes, the subunit RNA of these two viruses sedimented at an identical peak position of 36S (Fig. 2B). Therefore, the subunit size of genomic RNA of these two viruses appeared to be similar, i.e., a chain length of 10.5 kb as determined by electron microscopic measurements (11), and a complexity of about 11 kb as determined by fingerprint studies (2). The small difference in the sedimentation coefficient of the 60 to 70S dimer complexes of these two viruses may be due to configurational differences of the viral RNA.

The similarity of the subunit size and sequence complexity of these two viruses were also evident in the number of large T1 oligonucleotides seen in the fingerprints (Fig. 1A and C), i.e., 51 spots for Mo-MuLV$_{83}$ as compared with 53 spots for Mo-MuLV within the chain length range indicated by the two dye markers.

T1 oligonucleotide map of Mo-MuLV$_{83}$ and Mo-MuLV RNA. The fingerprints of poly(A)-containing RNA fragments of different size ranges are presented in Fig. 4 for Mo-MuLV$_{83}$ and in Fig. 5 for Mo-MuLV RNA. The poly(A)-containing RNA fractions were prepared from RNA randomly degraded (Fig. 3). Oligonucleotides that were strongly present in each individual fingerprint were numbered. The oligonucleotide map was constructed first by inspecting these fingerprints for full recovery as compared with the reference total RNA of each individual oligonucleotide in different size ranges of poly(A)-containing RNA fragments. In Mo-MuLV$_{83}$ RNA, T1 oligonucleotides such as 22a, 13, 1, 14a, A5, 2, 50b, 4, 10, and 8, which are present in the 26S fraction but completely or partially lost in the 22S fraction, were placed at a location close to the 5′ end. The same procedure was applied to other, smaller RNA fractions. The order of oligonucleotides within these groups was then determined by their relative molar yield in the second-dimension gels. Figure 6 presents data used to order the T1 oligonucleotides of the 3′ half of the viral genome. The lower relative molar yield of spot 18 in the 10S and 11S RNA fractions in Fig. 6 was due to loss of the 5′ counterpart of this terminally redundant oligonucleotide in less than full-length RNA fragments (J. M. Coffin and W. A. Haseltine, unpublished data). The order was much more certain at the 3′ half than at the 5′ half of the RNA molecules, since selection of RNA fragments was based on their 3′ poly(A) tracts. The major T1 oligonucleotides present in the 4S and 10S RNA fractions of Mo-MuLV$_{83}$ and the 6S and 13S fractions of Mo-MuLV were all com-

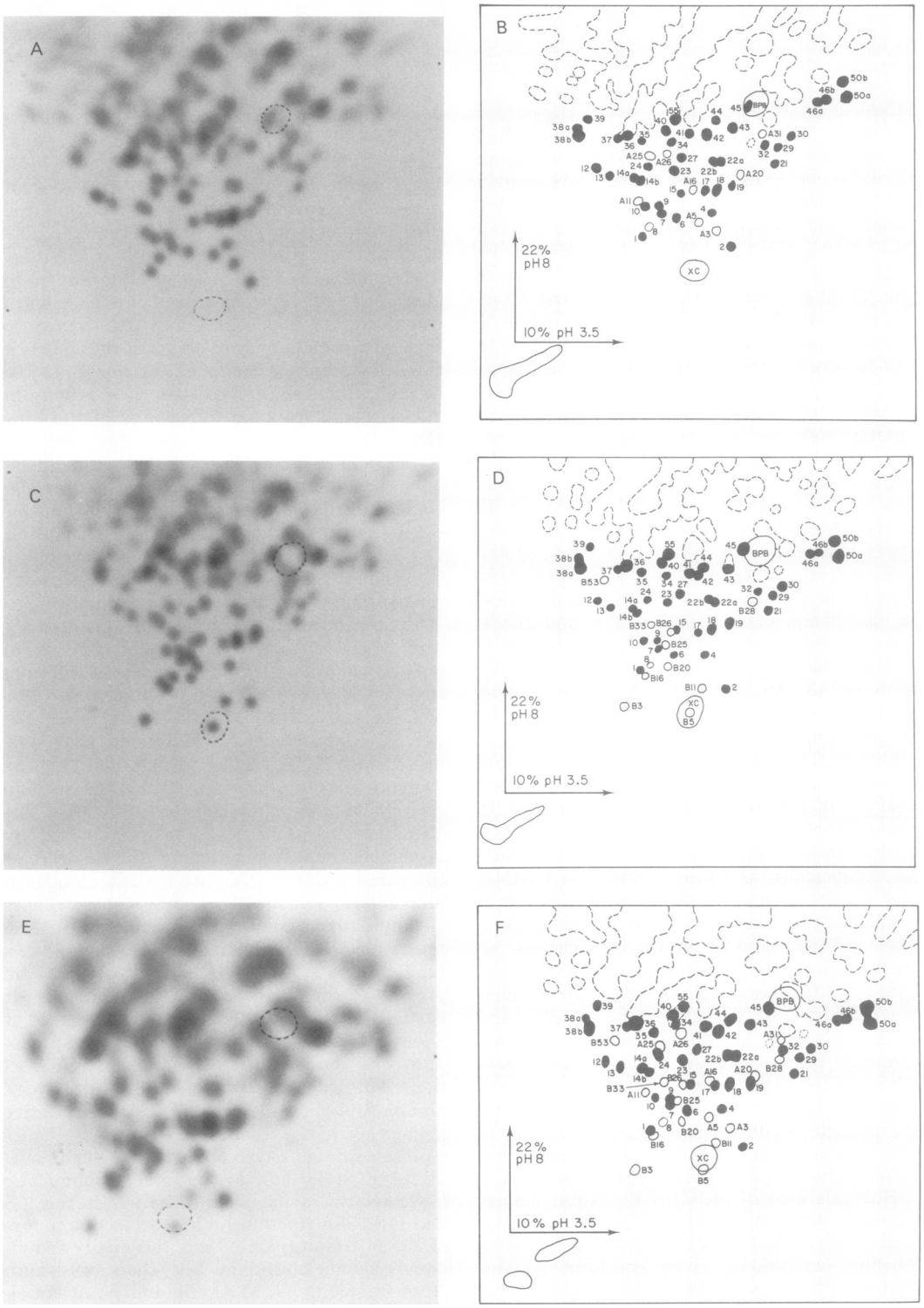

FIG. 1. *Comparison of fingerprints of Mo-MuLV$_{83}$ and Mo-MuLV RNA. [^{32}P]Mo-MuLV$_{83}$ RNA (1.2 × 10^6 cpm, 100 μg of yeast RNA), [^{32}P]Mo-MuLV RNA (1.2 × 10^6 cpm, 100 μg of yeast RNA) or a ratio of 1:1 cpm of both RNAs (1.5 × 10^6 cpm, 100 μg of yeast RNA) was digested with 10 μl of RNase T1 (11 U). After mixing with two dye markers, xylene cyanol FF and bromophenol blue, it was applied to the first-dimension gel (160 by 380 by 2 mm of 10% acrylamide–6 M urea–0.025 M citric acid, pH 3.5), and electrophoresis was performed until xylene cyanol reached the 20-cm mark. A gel strip (1 by 22 cm) with this dye marker at the center was cut out, the second-dimension gel was made with 21.8% acrylamide and 0.04 M tris(hydroxymethyl)aminomethane (Tris) citrate (pH 8.0), and electrophoresis was terminated after the bromophenol blue marker reached the 16-cm mark. The bottom edge of the figures is the origin of the second-dimension gel. The poly(A) mark is at the*

TABLE 1. *Comparison of T1 oligonucleotides of Mo-MuLV$_{83}$ and Mo-MuLV RNA by double-isotope labeling and by their RNase A digestion products*

Mo-MuLV$_{83}$ oligonucleotide no.	^3H-^{32}P ratio[a]	Composition[b]
(A) Common between Mo-MuLV$_{83}$ and Mo-MuLV		
1	1.10	A_4U, AU, 3AC, 9C, 4U, AG
2	0.83	A_4U, A_2U, A_2C, 4C, 6U, G
4	0.91	AU, 2AC, 9C, 7U, G
6	1.20	A_4U, A_2U, A_2C, 7C, 6U, G
7	1.25	2AU, 3AC, 9C, 7U, G
9	1.25	A_3U, A_2C, AU, AC, 5C, 3U, G
10	0.86	A_4C, A_2U, 2AU, AC, 5C, U, G
12	0.57	
13	0.71	$2A_3C$, 7C, 3U, A_2G
14a	1.00	A_4C, 2AC, 7C, 3U, G
14b	0.79	A_2U, A_2C, 2AU, 3AC, 8C 4U, G
15	1.06	2AU, AC, 9C, 4U, AG
17	0.78	A_3C, A_2C, AU, AC, 9C, 8U, 2G
18	1.20	$2A_3C$, $2A_2U$, 2AU, AC, 19C, 16U, AG, 2G
19	1.17	A_2C, 2AU, 2AC, 4C, 6U, AG
21	0.90	A_3C, 2AU, 4C, 6U, AG
22a	1.08	2AC, 7C, 7U, A_2G
22b	1.05	2AC, 8C, 7U, AG
24	1.03	A_4C, AU, AC, 9C, 4U, AG
27	1.54	$2A_4N$, A_2C, 2AU, 2AC, 2C, 2U, 2G
29	1.03	3AU, AC, 3C, 3U, G
30	0.86	
35	0.68	A_2U, $2A_2C$, 4C, 2U, AG
37	1.10	AC, 8C, 3U, G
42	1.28	AC, 6C, 3U, G
46b	1.0	AU, 2C, 7U, A_4G
50b	1.18	AC, 3C, 6U, G
(B) Mo-MuLV$_{83}$ unique		
A3	0.07	A_2C, 2AU, AC, 7C 2U, G
A5	0.15	A_2U, AU, 14C, 3U, G
A11	0.19	$2A_2C$, AC, 9C, 2U, G
A16	0.35	7C, 2U, A_4N
A20	1.30	A_2U, AC, 5C, 6U, A_2G
A25	0.39	A_2C, 3AC, 7C, 3U, AG
A26	0.37	A_4N, A_3C, 2AC, 6C, 5U, G
A31	1.03	
8	0.63	$2A_2C$, 2AC, 11C, 3U, G

[a] [^3H]Mo-MuLV RNA (3×10^6 cpm) was mixed with [^{32}P]Mo-MuLV$_{83}$ RNA (0.5×10^6 cpm). Fingerprinting was performed as described in the legend to Fig. 1. T1 oligonucleotides were located by the ^{32}P label in the autoradiography and were eluted from the gel disks (5 mm in diameter) by incubation with 0.5 ml of water (5 μg of RNase A) at 35°C for 18 h. After rinsing the gel disks with another 0.5 ml of water, the combined portions were counted in Ready-Solv VI (Beckman) with liquid scintillation counter (Beckman). In oligonucleotide no. 1 for example, ^3H was 2,115 cpm and ^{32}P was 325 cpm. The ^3H-^{32}P ratios were normalized by dividing with the input ^3H-^{32}P ratio of 5.92.

[b] [^{32}P]Mo-MuLV$_{83}$ RNA (14×10^6 cpm) was fingerprinted, and 5-mm disks were excised from the second-dimension gel. T1 oligonucleotides (20,000 to 5,000 cpm) were eluted by incubation with 0.5 ml of water (30 μg of yeast RNA) at 4°C for 48 h. Portions were removed and gel disks were rinsed with another 0.3 ml of water (20 μg of yeast RNA). The combined portions were lyophilized. Composition of pancreatic RNase A digests was analyzed as described by Coffin and Billeter (3). Common oligonucleotides possess compositions similar to those of Mo-MuLV, clone 1 (6, 14) analyzed by Coffin et al. (unpublished data). Numbers 37, 35, 42 and 50b of Mo-MuLV were not analyzed. Number 18 is a mixture of three oligonucleotides including two terminally redundant oligonucleotides.

left lower corner. Autoradiography was carried out with Kodak No-Screen X-ray films for 2 to 4 days at 4°C. T1 oligonucleotides were identified by superimposition of fingerprints. The unique spots were assigned with the "A" series number for Mo-MuLV$_{83}$ and "B" series number for Mo-MuLV except no. 8. The common spots were designated by the same number. (A) Mo-MuLV$_{83}$ RNA; (B) sketch of (A); (C) Mo-MuLV RNA; (D) sketch of (C); (E) equal counts per minute mixture of Mo-MuLV$_{83}$ and Mo-MuLV RNA; (F) sketch of (E).

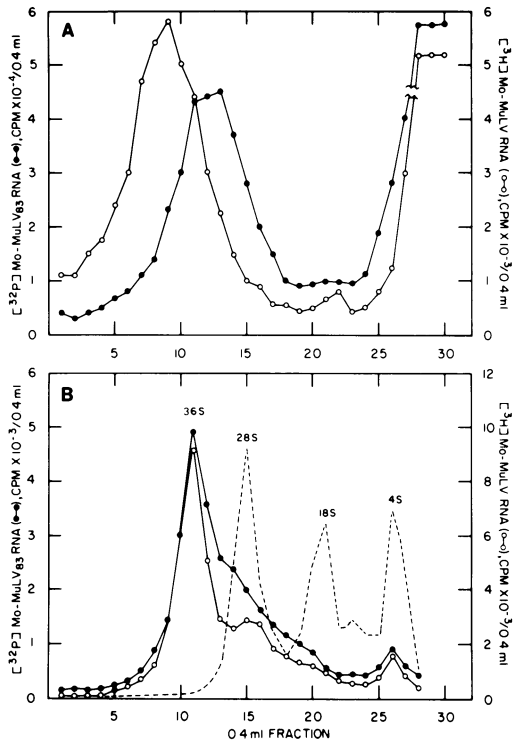

FIG. 2. *Sedimentation of [^{32}P]Mo-MuLV$_{83}$ and [^{3}H]Mo MuLV RNA in sucrose density gradients. (A) 70S RNA. A confluent culture of Mo-MuLV$_{83}$ on mink cells in a 150-cm^2 Falcon flask was labeled with 12 ml of phosphate-free medium supplemented with 1.5 Ci of [^{32}P]orthophosphate per ml. Mo-MuLV on SC-1 cells was labeled with 12 ml of complete medium with 0.1 Ci of [5-^{3}H]uridine (28 Ci/mmol) per ml for 20 h. A 6-ml portion of [^{32}P]Mo-MuLV$_{83}$ medium and 1 ml of [^{3}H]Mo-MuLV medium were combined, and viruses were pelleted at 29,000 rpm with a Spinco no. 30 rotor for 3 h (4°C) through 20% sucrose in TNE buffer (0.01 M Tris, pH 7.4–0.1 M NaCl–1 mM ethylenediamine-tetraacetic acid [EDTA]). The virus pellet was lysed in 1 ml of 1% sodium dodecyl sulfate and 0.2% (vol/vol) diethylpyrocarbonate in the TNE buffer. It was then layered on the 15 to 30% sucrose gradient in TNE buffer in an SW41 centrifuge tube. Centrifugation was at 39,000 rpm for 2.5 h at 20°C. Fractions of 0.4 ml were collected from the bottom of the tubes, and ^{3}H or ^{32}P radioactivity was counted after precipitation of the RNA with 25% trichloroacetic acid. (B) Subunit RNA. Mo-MuLV$_{83}$ was labeled with [^{32}P]orthophosphate, Mo-MuLV was labeled with [^{3}H]uridine, and 60 to 70S viral RNA was prepared as in (A). The only exception was that cells were first prelabeled overnight and media were collected twice at a 4-h interval. [^{32}P]Mo-MuLV$_{83}$ (53,000 cpm) and [^{3}H]Mo-MuLV (57,000 cpm) RNA were then combined and heat denatured at 80°C for 2 min in 300 μl of water. It was sedimented in a 15 to 30% sucrose gradient in TNE buffer in an SW41 rotor at 39,000 rpm for 6.5 h at 15°C. The [^{3}H]rRNA marker (65,000 cpm) was sedimented in a parallel gradient on the same rotor. Fractions of 0.45 ml were collected from the bottom of the tubes, and ^{3}H or ^{32}P radioactivity was counted after precipitation with 25% trichloroacetic acid.*

mon oligonucleotides, i.e., 12, 18, 35, 27, 14b, 29, 6, 46b, 15, and 24. In fact, the fingerprints of these two smallest RNA fractions were directly superimposable between these two viruses (see Fig. 5G and H). These results strongly indicate a substantial region of a common identical sequence at the 3′ end of the viral RNA molecules. Of special interest to note in the fingerprints of these poly(A)$^+$ RNAs as shown in Fig. 4 and 5 is the concurrent appearance of most of the unique T1 oligonucleotides in the 17S or 20S RNA fractions. In Mo-MuLV$_{83}$, there were no unique T1 spots in the 4S or 10S RNA, but in the 17S RNA, most of the unique spots such as A3, A11, A20, A25, A16, A31, and A26 were all visible except spots A5 and 8, which were apparently located close to the 5′ end of the RNA molecules. In the Mo-MuLV RNA, unique spots such as B28, B20, B3, B33, B53, B25, B26, B16, B11, and B5 all appeared concurrently in the 20S RNA. These results indicate clustering of unique spots within this region of viral RNA. The entire T1 oligonucleotide map of these two viral RNAs is seen in Fig. 7. The T1 oligonucleotide order was arranged primarily according to Mo-MuLV$_{83}$ fingerprints, and it was generally in good agreement with results obtained with Mo-MuLV. Some small discrepancy in the order of these two viruses as deduced from present data was most likely due to experimental uncertainty; these oligonucleotides are included within each bracket shown in Fig. 7. In Fig. 1, there were a total of 51 to 53 large T1 oligonucleotides in size range between the two dye markers, which represented approximately 10% of total RNA sequences. In view of the relatively large number of marker T1 oligonucleotides resolved in the fingerprints, it is quite reasonable to assume that these marker oligonucleotides represent a random sampling of the viral genome. There were 10 T1 oligonucleotides immediately adjacent to the 3′ poly(A) termini before any unique spots became evident; these oligonucleotides represented a stretch of approximately 2 kb (10/52 × 10.5) of common nucleotide sequences between these two viruses. In Mo-MuLV$_{83}$, the noncommon region ranged from oligonucleotides A3 to A26 in the map (Fig. 7) and represented 1.6 kb (8/52 × 10.5) of the genomic RNA. Similarly, the noncommon region appeared to be approximately 2.2 kb (11/52 × 10.5) in the Mo-MuLV genome. The calculation appeared to be more reasonable based on the total number of 52 oligonucleotides seen in Fig. 1 than on the 36 to 38 oligonucleotides included in the Fig. 7

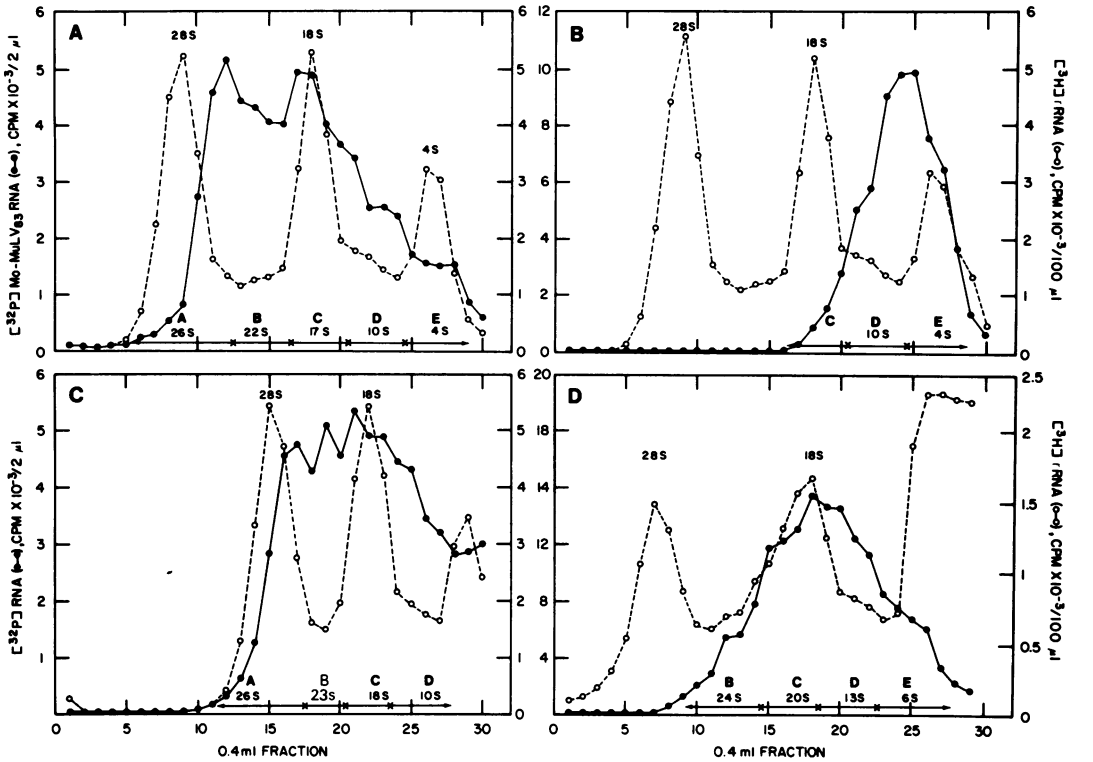

FIG. 3. *Sedimentation profiles of [^{32}P]Mo-MuLV$_{83}$ or [^{32}P]Mo-MuLV RNA fragments from which poly(A)$^+$ RNA has been selected. 60 to 70S viral RNA samples after heat dissociation at 95°C for 30 s were sedimented in a 10 to 25% sucrose gradient (0.01 M Tris [pH 7.2]-0.01 M NaCl-1 mM EDTA-0.1% sodium dodecyl sulfate) at 39,000 rpm in SW41 rotor (20°C) for 5.5 or 6.5 h. (A) [^{32}P]Mo-MuLV$_{83}$ RNA (19 × 10^6 cpm), naturally degraded. (B) [^{32}P]Mo-MuLV$_{83}$ RNA (19 × 10^6 cpm) further degraded by Na_2CO_3 treatment (0.05 M at 50°C for 6 min). (C) [^{32}P]Mo-MuLV RNA (20 × 10^6 cpm), naturally degraded. (D) [^{32}P]Mo-MuLV RNA (40 × 10^6 cpm) further degraded by Na_2CO_3 treatment (0.05 M at 50°C, 2 min). The [^{3}H]rRNA marker was sedimented in a parallel gradient on the same rotor. RNA fractions were pooled as indicated in the figure and purified by two cycles of oligo(dT)-cellulose chromatography (17, 23). The recovery of the poly(A)$^+$ RNA from the column was as follows: 26S fraction, 40%; 22S fraction 26%; 17S fraction, 22%; 10S fraction, 5%; and 4S fraction, 5%.*

map, since most of the uncertain spots not included were at the 5′ half of the RNA molecules. Figure 9 shows schematic structures of these two viral genomes. The common oligonucleotides such as no. 42 located within the substituted region may represent some conserved sequences in this portion of viral genome among MuLV's. The lone noncommon oligonucleotides A5 and 8 of Mo-MuLV$_{83}$ located at the 5′ part of viral RNA were most likely due to minor base variation between these two viruses, which were cloned from separate stocks of Mo-MuLV.

The location of noncommon sequences from approximately 2 to 3.6 or 4.2 kb away from the 3′ end as deduced from distribution of marker oligonucleotides was in good agreement with the first concurrent appearance of these unique spots in the 17S or 20S poly(A)$^+$ RNA fraction. The molecular length of the 18S RNA was 2.1 kb according to the following formula: molecular weight = 1,550 · $S^{2.1}$ (18, 23).

Hybridization of cDNA$_{SFFV}$ to Mo-MuLV$_{83}$ RNA. In an attempt to relate the noncommon sequences detected in Mo-MuLV$_{83}$ to the xenotropic sequences incorporated into the Friend strain of the SFFV, [^{32}P]Mo-MuLV$_{83}$ RNA was hybridized to cDNA$_{SFFV}$ and subsequently treated with a combination of pancreatic RNase A and RNase T1. The protected [^{32}P]Mo-MuLV$_{83}$ RNA was fingerprinted. Figure 8 shows the cDNA$_{SFFV}$-protected spots remaining in the fingerprint. By superimposition with a fingerprint of the total [^{32}P]Mo-MuLV$_{83}$ RNA obtained in parallel, one of the most intense spots overlapped with no. A11. A faint presence of A25, A16, and A31 was also visible in the original autoradiograph. In addition to these unique spots, some common oligonucleotides were also

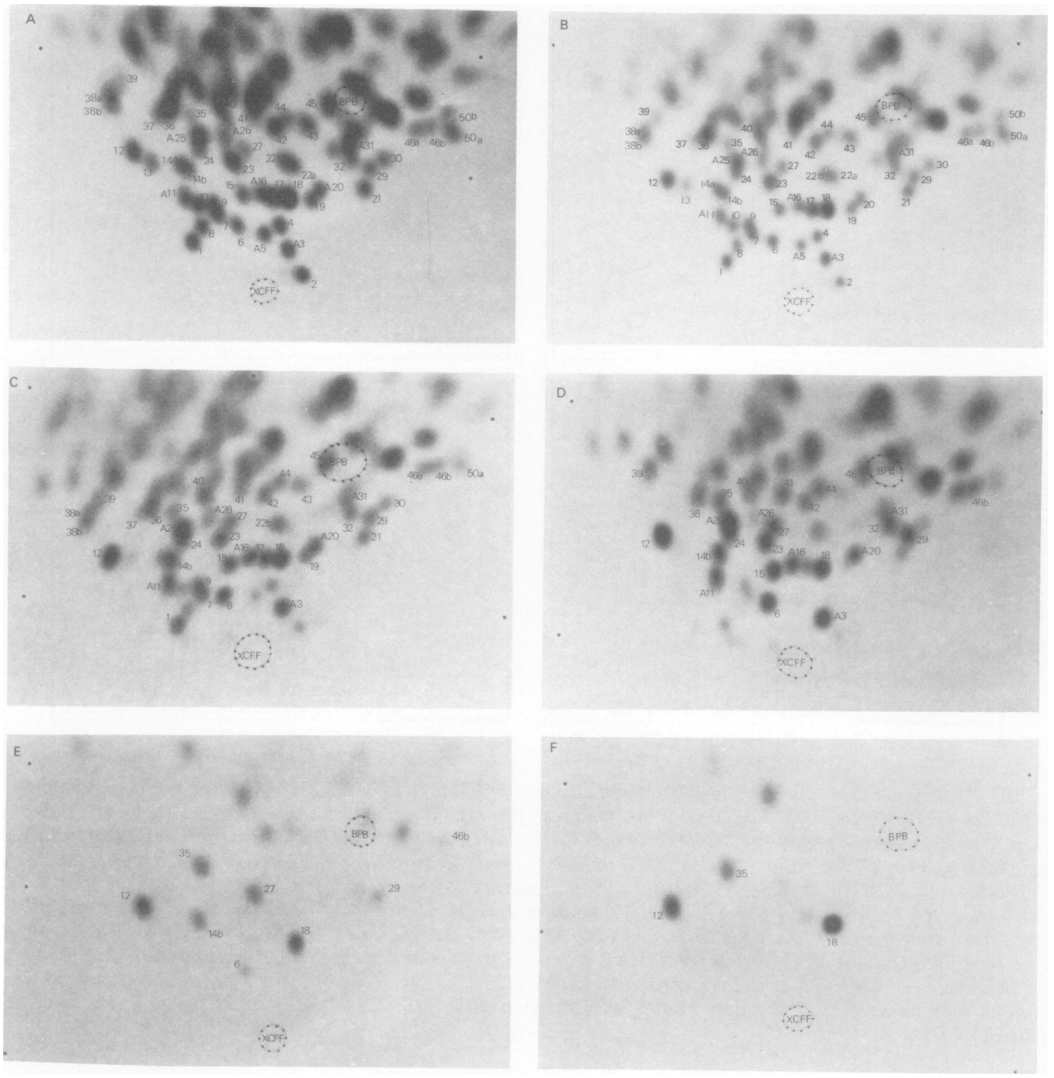

FIG. 4. *Fingerprints of Mo-MuLV$_{83}$ poly(A)$^+$ RNA fragments of different sizes. Poly(A)$^+$ RNA fragments pooled and purified by oligo(dT)-cellulose chromatography as shown in Fig. 3A and B were fingerprinted. (A) Total RNA without oligo(dT)-cellulose selection, 700,000 cpm. (B) 26S fraction (Fig. 3A), 464,000 cpm. (C) 22S fraction (Fig. 3A), 460,000 cpm. (D) 17S fraction (Fig. 3A), 442,000 cpm. (E) 10S fraction (Fig. 3B), 192,000 cpm. (F) 4S fraction (Fig. 3B), 149,000 cpm. Autoradiography was for 3 to 4 days. Oligonucleotides that were strongly present in each fingerprint were numbered.*

visible, probably due to contamination by helper leukemia viral sequences in this cDNA preparation used in the present hybridization experiment. The lone noncommon spots A5 and 8, which were located at the 5′ half, were not among those protected by cDNA$_{SFFV}$. Thus, it is most likely that the clustered unique spots extending from A3 to A26 represent the sequences complementary to cDNA$_{SFFV}$ and are the portion of the xenotropic sequences recombined with the Mo-MuLV RNA. The present observation agrees extremely well with earlier hybridization studies of cDNA$_{SFFV}$ to various-size poly(A)$^+$ RNA fragments of Mo-MuLV$_{83}$. cDNA$_{SFFV}$ hybridized more rapidly to the 18S and 26S than to the 35S, 12S, and 4S RNA fractions. As seen above, the cDNA$_{SFFV}$-protected unique spots all appeared concomitantly in the 17S poly(A)$^+$ RNA of [^{32}P]Mo-MuLV$_{83}$ RNA.

DISCUSSION

A detailed genetic map of mammalian RNA tumor viruses is still lacking. In the present paper, we have exploited the broadened host

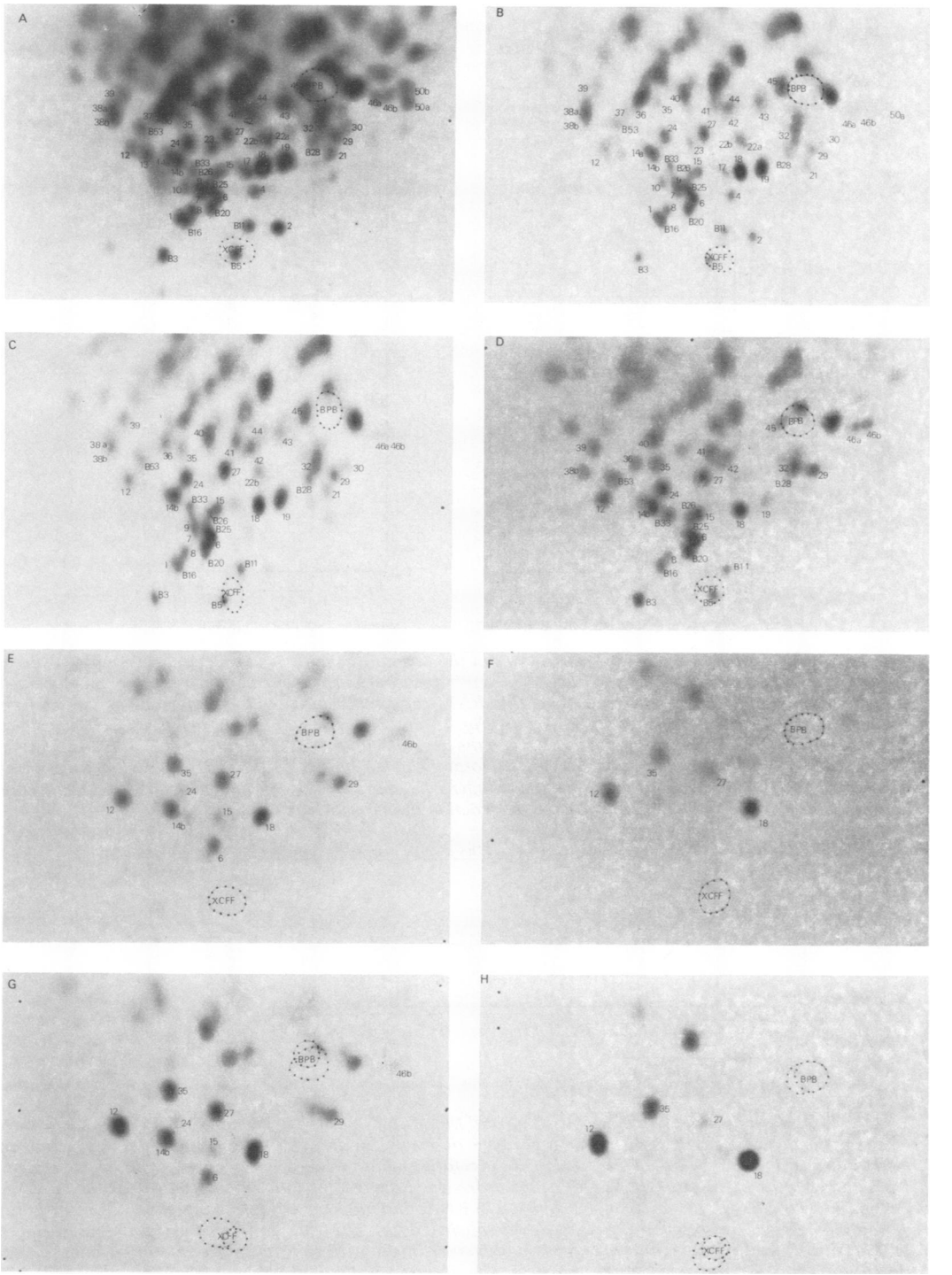

FIG. 5. *Fingerprints of Mo-MuLV poly(A)$^+$ RNA fragments of different sizes. Poly(A)$^+$ RNA fragments pooled and purified by oligo(dT)-cellulose chromatography as shown in Fig. 3C and D were fingerprinted. (A) Total RNA without oligo(dT)-cellulose selection (1.5 × 10^6 cpm). (B) 26S fraction (Fig. 3C), 400,000 cpm. (C) 23S fraction (Fig. 3C), 300,000 cpm. (D) 20S fraction (Fig. 3D), 500,000 cpm. (E) 13S fraction (Fig. 3D), 500,000 cpm. (F) 6S fraction (Fig. 3D), 250,000 cpm. Fingerprint of an 18S fraction (Fig. 3C) without Na_2CO_3 treatment was very similar to that of the 20S fraction (Fig. 3D) degraded by Na_2CO_3 (data not shown). Autoradiography was for 1 to 4 days. (G) Superimposition of fingerprints of the 13S Mo-MuLV RNA (this figure) and 10S Mo-MuLV$_{83}$ RNA (Fig. 4E). (H) Superimposition of fingerprints of the 6S Mo-MuLV RNA (this figure) and the 4S Mo-MuLV$_{83}$ RNA (Fig. 4F). Oligonucleotides that were strongly present in each fingerprint were numbered.*

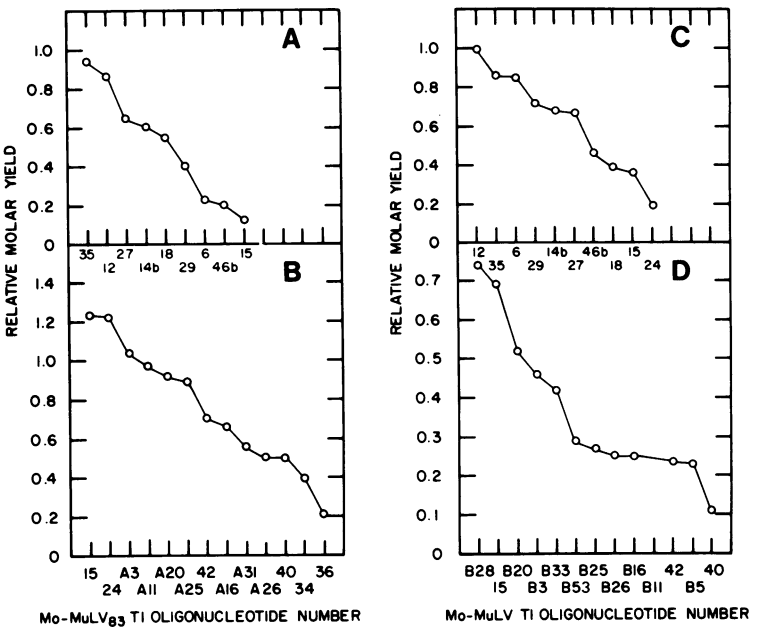

FIG. 6. *Relative recovery of T1 oligonucleotides in the second-dimension gels. The relative molar yield of the major spots in the second-dimension gels was determined by the ratio of counts per minute of gel disks (8 or 6 mm in diameter) of the gels of various poly(A)$^+$ RNA fragments relative to those of gel disks excised from corresponding spots of the control total RNA gels (Fig. 4A and 5A). The ratio of radioactivity (relative molar yield) presented in this figure was not normalized to the absolute molar ratio. The order of T1 oligonucleotides was arranged according to the decreasing relative molar yield. (A) 10S Mo-MuLV$_{83}$ RNA fraction (fingerprint, see Fig. 4E). (B) 17S Mo-MuLV$_{83}$ RNA fraction (fingerprint, see Fig. 4D). (C) 13S Mo-MuLV RNA fraction (fingerprint, see Fig. 5E). (D) 20S Mo-MuLV RNA fraction (fingerprint, see Fig. 5D).*

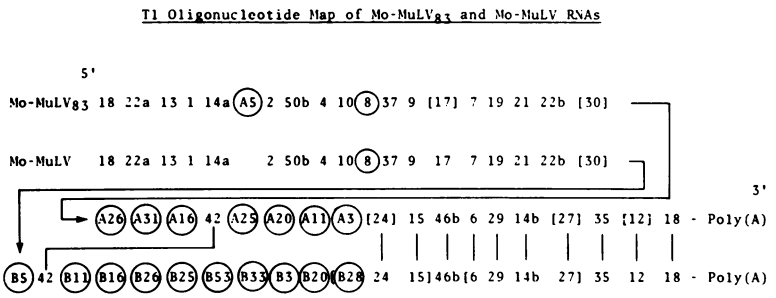

FIG. 7. *T1 oligonucleotide map of Mo-MuLV$_{83}$ and Mo-MuLV 70S RNA. The order of T1 oligonucleotides in the map was deduced by a two-step procedure described in the text involving visual inspection of fingerprints in Fig. 4 and 5 and determination of the relative molar yield of T1 oligonucleotides in the second-dimension gels (Fig. 6). In Mo-MuLV$_{83}$ RNA, the order was arranged as follows: no. 18 to 35 by the 4S RNA; no. 27 to 46b by the 10S RNA; no. 15 to A26 by the 17S RNA; and no. 30 to 22a by the 22S RNA. The terminally redundant no. 18 was by Coffin and Haseltine (unpublished data). The order presented was primarily deduced from Mo-MuLV$_{83}$ fingerprints, and the common oligonucleotides with slight variation in order found in Mo-MuLV fingerprints are included in the brackets. The accuracy of the location of a few Mo-MuLV$_{83}$ oligonucleotides in brackets may be less than that of others due to impurities found in composition analysis (Table 1). All the unique oligonucleotides between these two viruses are circled.*

range and changes in the *env* gene function of a recombinant virus between Mo-MuLV and a xenotropic virus in an attempt to map the location of *env* gene within the Mo-MuLV genome. By studying fingerprints of RNase T1-resistant oligonucleotides of Mo-MuLV$_{83}$ and Mo-MuLV RNA, it became apparent that the genomic RNA of these two viruses shared 42 out of 52 T1 oligonucleotides, indicating that approximately 80% of the viral genome is composed of the same

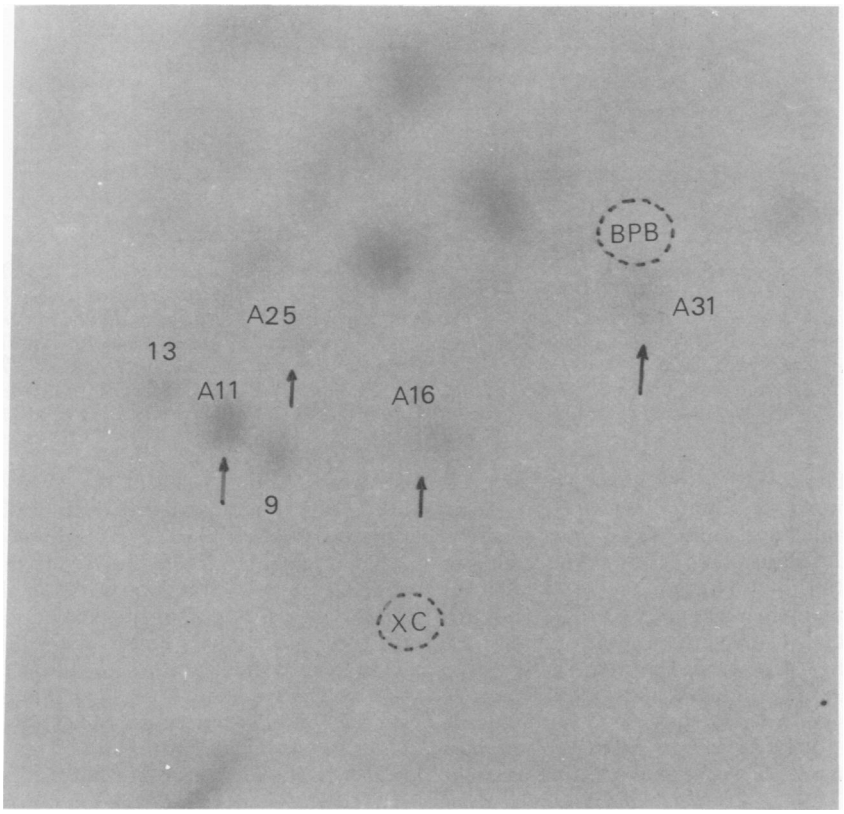

FIG. 8. *Hybridization of cDNA$_{SFFV}$ to [^{32}P]Mo-MuLV$_{83}$ RNA. [^{3}H]cDNA$_{SFFV}$ (1 × 10^{6} cpm, ca. 0.1 μg) was hybridized to [^{32}P]Mo-MuLV$_{83}$ RNA (2.4 × 10^{6} cpm, ca. 1 μg) in 50 μl of 0.5 M NaCl–0.05 M Tris-hydrochloride (pH 7.2) at 65°C for 20 h. In addition, 22 μg of unlabeled F-MuLV RNA was included to suppress the background hybridization of the helper leukemia viral sequences. At the end of incubation, the unhybridized [^{32}P]RNA was digested with a mixture of RNase A (5 μg) and RNase T1 (4 U) at 37°C for 30 min. After inactivation of RNase by 0.2% diethylpyrocarbonate, the digested RNA was then removed by passage through a Sephadex G75 column. The protected [^{32}P]Mo-MuLV$_{83}$ RNA was pooled from the void fractions. The [^{32}P]-RNA-cDNA hybrid was extracted by phenol-chloroform (50:50) and was precipitated by 2.5 volumes of ethanol. After dissolving the RNA hybrid in 150 μl of water, it was dissociated by heating at 95°C for 30 s and lyophilized. After further digestion with 10 μl of RNase T1 solution (11 U) at 35°C for 30 min, the protected ^{32}P-labeled oligonucleotides were fingerprinted. The trichloroacetic acid-precipitable [^{32}P]RNA remaining after hybridization and digestion with RNase A and T1 was about 5% of the total input as determined by a 2% portion of the sample. Autoradiography was for 17 days at 4°C.*

nucleotide sequences. The total length and complexity of these two viral RNAs also appeared to be the same. A cluster of 7 (in Mo-MuLV$_{83}$) or 10 (in Mo-MuLV) unique T1 oligonucleotides were mapped approximately 2 to 4 kb from the 3′ end of the viral RNA. Most likely, this is the location of the *env* gene region of the Mo-MuLV genome. However, with our present results we are unable to conclude whether this nonhomologous region alone represents the *env* gene or whether the gene border actually spans across this region and includes neighboring portions of the homologous sequences. The interference pattern in virus infection shows that Mo-MuLV$_{83}$ is interfered with by xenotropic and slightly by ecotropic viruses (21). It is possible that the *env* gene region includes part of the homologous region.

There still is no direct evidence for the location of other genetic functions of MuLV. However, the observation that in vitro translation products of the intact viral RNA are predominantly of the *gag* gene products suggests the 5′ location of the *gag* gene, assuming that the other internal initiation sites are silent (8, 14). This is also consistent with the faster hybridization kinetics of cDNA$_{gag}$ to the longest poly(A)-containing RNA fragments than with the hybridization kinetics of cDNA$_{SFFV}$ or cDNA$_{3'}$, which detects portions of the genome closer to the 3′

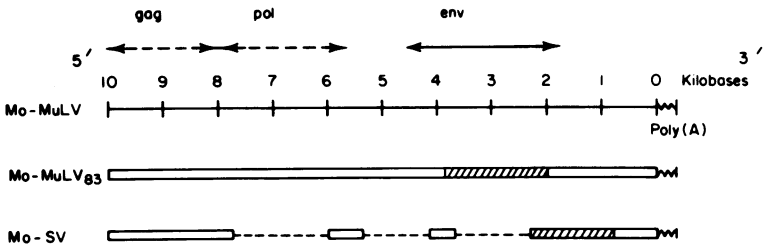

FIG. 9. *Comparison of the physical gene map of recombinant viruses derived from Mo-MuLV. The molecular length of Mo-MuLV genomic RNA of 10.5 kb including the poly(A) tract is as described by Hu et al. (11). The blank blocks of Mo-MuLV$_{83}$ and Moloney sarcoma virus (Mo-MuSV) indicate the homologous sequences of the parent Mo-MuLV retained in these derivatives, and the hatched blocks describe the new sequences acquired by Mo-MuLV$_{83}$ and Mo-MuSV. (----) Parental regions deleted in Mo-MuSV. The location of env gene is deduced from present results, and the location of gag and pol is inferred from other evidence discussed in the text. The Mo-MuSV map is reproduced from the heteroduplex data by Hu et al. (11).*

end (21). The Pr65 *gag* precursor (19) spans 2 kb in the nucleotide map. The location of the *pol* gene immediately after the *gag* gene is suggested by the occasional readthrough of the *gag* gene resulting in a *gag-pol* precursor with an approximate molecular weight of 200,000 (12). The Pr75RT precursor (12) requires at least 2.2 kb of coding capacity in the map. A tentative genetic map of Mo-MuLV is depicted in Fig. 9, with the gene order in the 5′ to 3′ direction of *gag-pol-env*-poly(A). It is of interest to compare the present results with the heteroduplex mapping data (11) of an S^+L^- Moloney sarcoma virus, which retains the *gag* gene product P30 but lacks complete polymerase and envelope gp70 (15, 16). In the map, most of the *pol* and *env* gene regions have been deleted. The substituted *sarc* sequences could have been derived from the *env* gene region of a yet unidentified parental endogenous mouse virus. The genetic map of Rous sarcoma virus as deduced by fingerprint studies of the viral RNA is as follows: the common sequence from 3′ poly(A) end to 0.6 kb; the *sarc* gene from 0.6 to 2 kb; the *env* gene from 2.5 to 5 kb; the *pol* gene from 6 to 8 kb; and the *gag* gene from 8 to 10 kb (5, 13). The present studies on Mo-MuLV place the location of *env* gene on almost the same location as that found in Rous sarcoma virus, and the general gene order appears to be similar to that of avian viruses. It is possible that all the RNA tumor viruses have evolved from a common ancestor prototype virus and that the gene order is conserved during evolution.

In the formation of the SFFV component of the Friend leukemia virus complex, a portion of xenotropic sequences has been incorporated into the Friend helper type C virus, and a probe designated as cDNA$_{SFFV}$ detects that portion of the xenotropic virus genome (20). cDNA$_{SFFV}$ protected at least four T1 oligonucleotides in the cluster of unique spots of Mo-MuLV$_{83}$. In another experiment, cDNA$_{SFFV}$ hybridized more rapidly with the 18S and 26S fraction of poly(A)$^+$ RNA fragments of Mo-MuLV$_{83}$ than with the 35S, 10S, and 4S fractions. Most of the unique spots concurrently appeared in the fingerprints in these fractions. These two observations strongly indicate that the same homologous portion of the xenotropic virus genome has undergone recombination with Friend type C helper virus in the formation of SFFV, or with Mo-MuLV in the formation of Mo-MuLV$_{83}$, or with AKR MuLV in the formation of AKR-MCF virus. In other words, the recombination appears to involve the same portion of the *env* gene region, and cDNA$_{SFFV}$ is a probe detecting the *env* gene region of xenotropic viruses. In AKR-MCF virus, the envelope glycoproteins have been shown to be recombinant molecules of ecotropic and xenotropic origin (6).

ACKNOWLEDGMENTS

We thank William Vass, Janice K. Boyars, and David Williams for excellent technical assistance, and Audrey Boyle for assistance in preparing this manuscript.

This work was supported by the Virus Cancer Program of the National Cancer Institute, and by Public Health Service grant CA17659 from the National Cancer Institute to J.M.C.

LITERATURE CITED

1. **Baltimore, D.** 1975. Tumor viruses: 1974. Cold Spring Harbor Symp. Quant. Biol. **39**:1187-1200.
2. **Beemon, K. L., A. J. Faras, A. T. Haase, P. H. Duesberg, and J. E. Maisel.** 1976. Genomic complexities of murine leukemia and sarcoma, reticuloendotheliosis and visna viruses. J. Virol. **17**:525-537.
3. **Coffin, J. M., and M. A. Billeter.** 1976. A physical map of the Rous sarcoma virus genome. J. Mol. Biol. **100**:293-318.
4. **Dina, D., K. Beemon, and P. Duesberg.** 1976. The 30S Moloney sarcoma virus RNA contains leukemia virus nucleotide sequences. Cell **9**:299-309.
5. **Duesberg, P. H., L. H. Wang, P. Mellon, W. S. Mason, and P. K. Vogt.** 1976. Towards a complete genetic map of Rous sarcoma virus, p. 107-125. *In* D. Baltimore, A.

Huang, and C. F. Fox (ed.), Proceedings of the ICN-UCLA Symposium on Animal Virology, vol. 4. Academic Press Inc., New York.

6. **Elder, J. H., J. W. Gautsch, F. C. Jensen, R. A. Lerner, J. W. Hartley, and W. P. Rowe.** 1977. Biochemical evidence that MCF murine leukemia viruses are envelope (*env*) gene recombinants. Proc. Natl. Acad. Sci. U.S.A. **74**:4676–4680.
7. **Fan, H., and M. Paskind.** 1974. Measurement of the sequence complexity of cloned Moloney murine leukemia virus 60 to 70S RNA: evidence for a haploid genome. J. Virol. **14**:421–429.
8. **Gielkens, A. L. J., D. Van Zaane, H. P. J. Bloemers, and H. Bloemendal.** 1976. Synthesis of Rauscher murine leukemia virus-specific polypeptide *in vitro*. Proc. Natl. Acad. Sci. U.S.A. **73**:356–360.
9. **Hanafusa, H.** 1975. Etiology-viral carcinogenesis. p. 49–90. *In* F. Becker (ed.), Cancer: a comprehensive treatise, vol. 2. Plenum Publishing Corp., New York and London.
10. **Hartley, J. W., N. K. Wolford, L. J. Old, and W. P. Rowe.** 1977. A new class of murine leukemia virus associated with development of spontaneous lymphoma. Proc. Natl. Acad. Sci. U.S.A. **74**:789–792.
11. **Hu, S., N. Davidson, and I. M. Verma.** 1977. A heteroduplex study of the sequence relationships between the RNAs of M-MSV and M-MuLV. Cell **10**:469–477.
12. **Jamjoom, G. A., R. B. Naso, and R. B. Arlinghaus.** 1977. Further characterization of intracellular precursor polyproteins of Rauscher leukemia virus. Virology **78**:11–34.
13. **Joho, R. H., E. Stoll, R. R. Friis, M. A. Billeter, and C. Weissman.** 1976. A partial genetic map of Rous sarcoma virus RNA: location of polymerase, envelope and transformation markers, p. 127–145. *In* D. Baltimore, A. Huang, and C. F. Fox (ed.), Proceedings of the ICN-UCLA Symposium on Animal Virology, vol. 4. Academic Press Inc., New York.
14. **Kerr, I. M., U. Olshevsky, H. F. Lodish, and D. Baltimore.** 1976. Translation of murine leukemia virus RNA in cell-free systems from animal cells. J. Virol. **18**:627–635.
15. **Parks, W. P., R. S. Howk, A. Anisowicz, and E. M. Scolnick.** 1976. Deletion mapping of Moloney type C virus: polypeptide and nucleic acid expression in different transforming virus isolates. J. Virol. **18**:491–503.
16. **Peebles, P. T., B. I. Gerwin, and E. M. Scolnick.** 1976. Murine sarcoma virus defectiveness: serological detection of only helper virus reverse transcriptase in sarcoma virus rescued from nonmurine S+L− cells. Virology **70**:313–323.
17. **Shih, T. Y., H. A. Young, J. M. Coffin, and E. M. Scolnick.** 1978. Physical map of the Kirsten sarcoma virus genome as determined by fingerprinting RNase T1-resistant oligonucleotides. J. Virol. **25**:238–253.
18. **Spirin, A. S.** 1963. Some problems concerning macromolecular structure of RNA. Prog. Nucleic Acid Res. Mol. Biol. **1**:301–345.
19. **Stephenson, J. R., S. R. Tronick, and S. A. Aaronson.** 1975. Murine leukemia virus mutants with temperature-sensitive defects in precursor polypeptide cleavage. Cell **6**:543–548.
20. **Troxler, D. H., J. K. Boyars, W. P. Parks, and E. M. Scolnick.** 1977. Friend strain of spleen focus-forming virus: a recombinant between mouse type C ecotropic viral sequences and sequences related to xenotropic virus. J. Virol. **22**:361–372.
21. **Troxler, D. H., D. Lowy, R. Howk, H. Young, and E. M. Scolnick.** 1977. The formation of an acute leukemia virus, the spleen focus-forming virus was accompanied by recombination between ecotropic murine type-C virus and the *env* gene region of xenotropic type-C virus. Proc. Natl. Acad. Sci. U.S.A. **74**:4671–4675.
22. **Vogt, P. K.** 1977. Genetics of RNA tumor viruses, p. 341–455. *In* H. Fraenkel-Conrat and R. R. Wagner (ed.), Comprehensive virology, vol. 4. Plenum Press, New York.
23. **Wang, L. H., P. Duesberg, K. Beemon, and P. K. Vogt.** 1975. Mapping RNase T1-resistant oligonucleotides of avian tumor virus RNAs: sarcoma specific oligonucleotides are near the poly(A) end and oligonucleotides common to sarcoma and transformation-defective viruses are at the poly(A) end. J. Virol. **16**:1051–1070.
24. **Wang, L. H., D. Galehouse, P. Mellon, P. Duesberg, W. S. Mason, and P. K. Vogt.** 1976. Mapping oligonucleotides of Rous sarcoma virus RNA that segregate with polymerase and group-specific antigen markers in recombinants. Proc. Natl. Acad. Sci. U.S.A. **73**:3952–3956.